Journal of Sound and Vibration (1998) **212**(5), 829–854

POWER TRANSMISSION BETWEEN TWO FINITE BEAMS AT LOW MODAL OVERLAP

C. T. HUGIN*

Department of Acoustic Technology, Technical University of Denmark, DK-2800 Lyngby, Denmark

(*Received* 27 *November* 1995, *and in final form* 19 *December* 1997)

The coupling loss factors frequently used in Statistical Energy Analysis are frequently based on a wave approach that assumes that the transmitted waves returning to the junction are uncorrelated with the directly transmitted waves. This assumption is generally not fulfilled for structures at low frequencies where the response exhibits distinctly well separated resonances. A method is presented here for calculation of an improved coupling loss factor for one-dimensional subsystems. By applying statistical considerations to an analytical expression for the net power transmission it is possible numerically to calculate an average value of the ratio of reflected to incident wave amplitude at the junction. From this ratio an improved coupling loss factor can be calculated which takes into account the re-radiation and re-injection of power which normally occurs between two reverberant fields. This improved coupling loss factor has the following features: it is valid at low modal overlap, it is independent of the exact boundary conditions, it depends upon the loss factor of the receiving subsystem, and its calculation is not dependent on the strength of the coupling. To illustrate the method, a specific beam system is considered in the frequency range where the modal overlap is small. Coupling loss factors are calculated and are employed in a traditional SEA model to predict mean square velocities for each beam element with good accuracy.

1. INTRODUCTION

Determination of the vibrational response of complex structures from deterministic models will normally result in lengthy calculations. Furthermore, the computational demands will increase greatly if the number of elements are increased or, in the case of numerical methods, if the response at higher frequencies is needed. Unfortunately, a quest for the exact response is rather vain as the structural response at higher frequencies is very sensitive to minor changes in details, especially with regard to the boundary conditions of the system. As a consequence, there will normally be considerable deviations between the predictions based on an exact deterministic model and the actual system response.

In order to reduce the computational efforts and to take into consideration the inherent uncertainties, methodical prediction frameworks have been developed such as the Statistical Energy Analysis (SEA) [1] and the mean value method (MVM) [2]. In such frameworks it is of utmost importance to include an adequate description of the power transmission between finite subsystems. Consequently, obtaining simplified descriptions of the power transmission between finite subsystems has been a subject for many investigations.

*Currently at ESDU International plc, London N1 6UA, U.K.

0022–460X/98/200829 + 26 $25.00/0/sv971472

bending waves. Analysis of such systems have traditionally employed either a modal approach [3–6], a wave approach [7–9] or the use of ensemble averages [10].

The present investigation is distinguished from previous analyses of similar two beam systems in that the starting point is in practice an exact analytical expression for the net transmitted power in a two-beam system subject to bending waves [11]. There are two key features of this analytical expression. First, the coupling between subsystems is described by reflection and transmission coefficients found from the analysis of the coupling between two semi-infinite systems. Second, this expression does not describe an average system having average mobilities (i.e., characteristic mobilities) but it describes a real system with natural frequencies and it does it exactly for the frequency range concerned here. The only approximation that has been made in deriving this expression is that it has been assumed that the influence of the near fields is negligible. This condition is normally fulfilled for frequencies above the first few natural frequencies of the system. Above the first two natural frequencies, predictions based on this expression are found to agree almost perfectly in all details with exact calculations.

In this paper it is demonstrated that the average ratio of reflected to incident wave amplitude from the second non-excited beam can be calculated as an average of the product of the so-called net reflection and the vibratory phase of the driven beam. This average ratio expresses the average absorption which in turn can be used to calculate an improved coupling loss factor to be used in a traditional SEA model. The improved coupling loss factor has two main benefits: it takes into consideration the effect of power being transmitted back to the emitting element and it is valid even at low modal overlap, a condition which so far has been beyond the reach of SEA. This improved coupling loss factor is independent of the exact boundary conditions of the elements but depends on the loss factor of the receiving beam. Also, the suggested approach is not restricted to cases of either weak coupling or strong coupling. The definition of weak coupling is the one given by Langley [12]: that of the Green function of the coupled subsystem being approximately equal to the Green function of the uncoupled subsystem.

To illustrate the method, a specific system of coupled beams is considered in the low frequency range with low modal overlap. Improved coupling loss factors are calculated for the couplings and these are then employed in a SEA model to predict the mean square velocities of each beam. The predicted mean square velocities are found to have a good agreement with exact calculation results as they are generally within ± 2 dB of these. Finally, the values of the improved coupling loss factors are compared to analytical expressions for coupling loss factors given in the literature.

2. POWER TRANSMISSION

The system examined is depicted in Figure 1. It consists of two coupled Euler–Bernoulli beams of finite lengths l_1 and l_2 in which only bending waves are present. The subscripts 1 and 2 refer to the driven beam and the receiving beam, respectively. The properties of the extreme non-coupled boundaries and the joint or coupling are given by reflection and transmission coefficients [13] as indicated. Here for example t_{12} is the transmission coefficient from beam 1 to beam 2. For the case shown where beam 1 is driven at the position x_0 (>0) by a harmonic point force F_0, the net transmitted power P_1 in the driven beam at position x_1 to the right of the force position x_0 will be given by [11]

$$P_1(x_1) \simeq \frac{|F_0|^2 |e^{jk_1 x_0} + r_0 e^{-jk_1 x_0}|}{16 m_1' c_{B_1}} \frac{|e^{-jk_1 x_1}|^2 - |R_1 e^{-jk_1(2l_1 - x_1)}|^2}{|1 - r_0 R_1 e^{-jk_1 2l_1}|^2}, \qquad x_0 > 0, \tag{1}$$

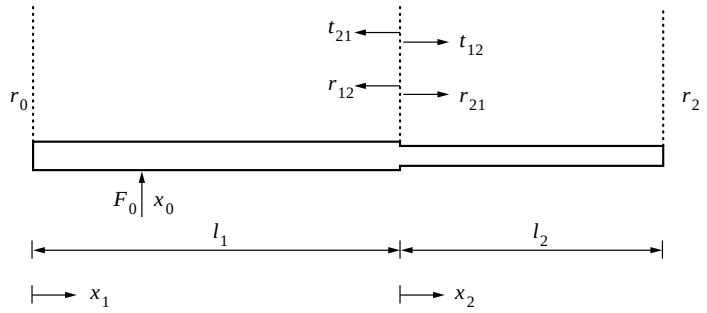

Figure 1. System consisting of two coupled finite beams with reflection and transmission coefficients. The first beam is driven by a harmonic point force F_0 at $x_1 = x_0$. The boundary conditions at the extreme ends and the properties of the coupling at $x_1 = l_1$ are given by their reflection and transmission coefficients.

where m_1' is the mass per length, c_{B_1} the phase velocity of bending waves, k_1 is the wave number, and r_0 is the reflection coefficient corresponding to the boundary condition at the left end of beam 1. Underlining of the wave number k indicates that damping is taken into account by employing a complex wave number, i.e., $\underline{k} \approx k(1 - j\eta/4)$ where η is the loss factor. The quantity R_1 is the so-called net reflection given by

$$R_1 = r_{12} + t_{12}t_{21}r_2/(e^{ik_2 2l_2} - r_{21}r_2), \tag{2}$$

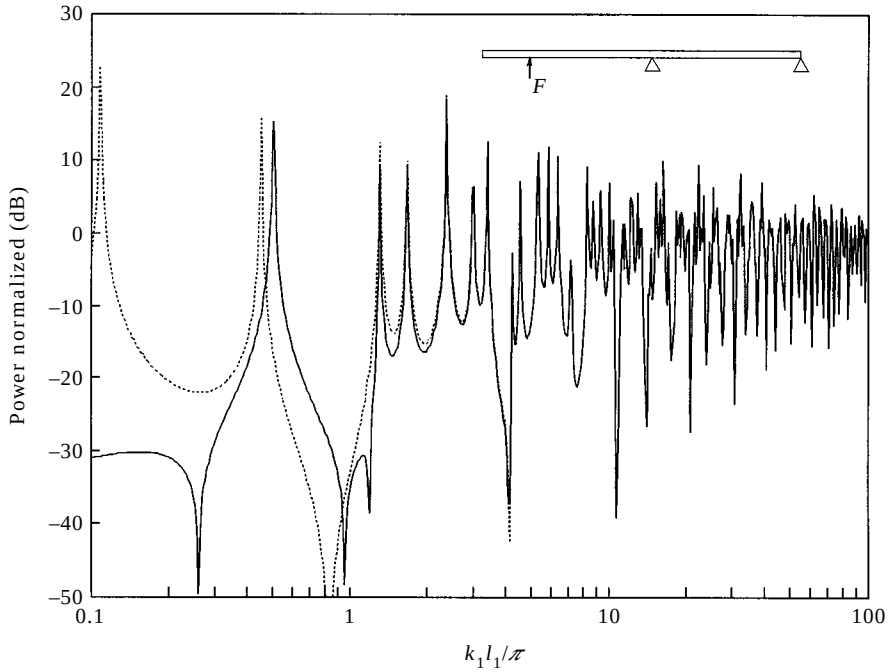

Figure 2. Net transmitted power in driven beam at $x_1/l_1 = 0{\cdot}6$ when driven by a harmonic force in position $x_0/l_1 = 0{\cdot}3$. Systems consisting of two coupled beams with $k_1 = k_2$. The left end is free, the coupling is a simple support and the left end is simply supported: ——, Exact calculation; ——, equation (1). Loss factor $\eta = 0{\cdot}01$.

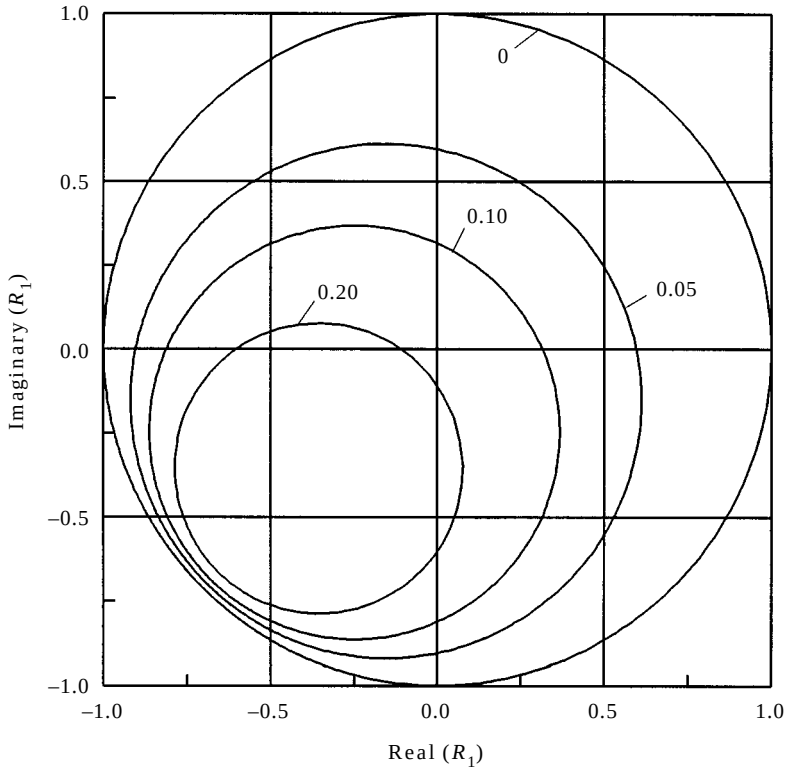

Figure 3. Nyquist plot of net reflection R_1 as a function of $k_2 2l_2$ for different values of the damping in the second beam, expressed by the parameter $k_2 l_2 \eta/4$ in the figure. The system consists of two beams coupled via a simple support; the beams have identical wave numbers $k_1 = k_2$ and beam 2 has a reflection termination $|r_2| = 1$.

where r_{12}, r_{21}, t_{12}, t_{21} are the reflection and transmission coefficients of the coupling, and r_2 is the reflection coefficient of the right end of beam 2. The reflection and transmission coefficients in equations (1) and (2) can equally well be those for amplitude waves as those for power waves [14].

In deriving equations (1) and (2) it has been assumed that the contribution of the reflected near fields is negligible. This corresponds to assuming that

$$e^{-k_1 x_0} \approx 0, \qquad e^{-k_1(l_1 - x_0)} \approx 0, \qquad e^{-k_2 l_2} \approx 0. \tag{3a–c}$$

If the position x_0 is chosen to be not too close to one of the ends of beam 1 then the conditions given by equations (3) will normally be fulfilled at frequencies higher than the first or second natural frequency of the system. This is illustrated in Figure 2 which shows a comparison between the net transmitted power P_1 calculated exactly and approximately by using equation (1). Above the second natural frequency of the system, it is seen that the approximation coincides almost perfectly with the exact calculation because the errors are of the orders: $\exp(-k_1 x_0)$, $\exp(-k_2 l_2)$ and $\exp(-k_1(l_1 - x_0))$.

If beam 1 were free at its left end, i.e., at $x_1 = 0$, and if it also were driven at this position then the net transmitted power in the driven beam would be given by [11]

$$P_1(x_1) \simeq \frac{|F_0|^2}{2m_1' c_{B_1}} \frac{|e^{-j\underline{k}_1 x_1}|^2 - |R_1 e^{-j\underline{k}_1(2l_1 - x_1)}|^2}{|j - R_1 e^{-j\underline{k}_1 2l_1}|^2}, \tag{4}$$

where the net reflection R_1 is still given by equation (2). In this case the errors will be of orders $\exp(-k_1 l_1)$ and $\exp(-k_2 l_2)$.

Equations (1) and (4) describe the net power transmission P_1 in beam 1 from knowledge of the Helmholtz numbers ($k_1 l_1$ and $k_2 l_2$), the reflection and transmission coefficients of the coupling (joint) and the non-coupled ends. The influence of beam 2 on beam 1 is given by the complex quantity: the net reflection R_1. The modulus of R_1 describes indirectly the power absorbed in beam 2. As can be seen from equation (2), when losses are present in beam 2 (the coupling loss factor $\eta_2 > 0$) then the modulus of R_1 will vary with frequency, or more precisely, with the Helmholtz number $k_2 l_2$.

The purpose of the first part of this investigation is to calculate the average influence of beam 2 on beam 1, expressed as the average ratio of reflected wave amplitude from the junction to incident wave amplitude on the junction. From equations (1) and (4) it can be seen that the level of the net power transmission at resonance is dominated by the denominator. As $|R_1|$ varies only slowly with frequency it is mainly the phase θ of $R_1 \exp(-\mathrm{j}k_1 2l_1)$, $\theta = \arg(R_1 \exp(-\mathrm{j}k_1 2l_1))$, that determines the magnitude of the net transmitted power. As $|R_1 \exp(-\mathrm{j}k_1 2l_1)|$ expresses the ratio of reflected wave to incident wave amplitudes, the phase θ is chosen to be the independent variable and $|R_1 \exp(-\mathrm{j}k_1 2l_1)|$ as the dependent variable. This is on the assumption that the ratio of the Helmholtz numbers for the two beams N $(=k_1 l_1/k_2 l_2)$ is known, in which case $|R_1 \exp(-\mathrm{j}k_1 2l_1)|$ can be expressed as a function of the phase θ. The product $R_1 \exp(-\mathrm{j}k_1 2l_1)$ can then be rewritten as

$$R_1 \, \mathrm{e}^{-\mathrm{j}k_1 2l_1} = |R_1(\theta)| \, \mathrm{e}^{-\mathrm{j}\theta}, \qquad \theta = \arg(R_1 \, \mathrm{e}^{-\mathrm{j}k_1 2l_1}) = \varphi_R - k_1 2l_1 = \varphi_R - Nk_2 2l_2, \quad (5\mathrm{a, b})$$

where $\varphi_R = \arg(R_1)$ and R_1 depends on $k_1 2l_1$. It should be noted that in equation (1), it is assumed that r_0 is a constant, although this need not be the case in general. Choosing

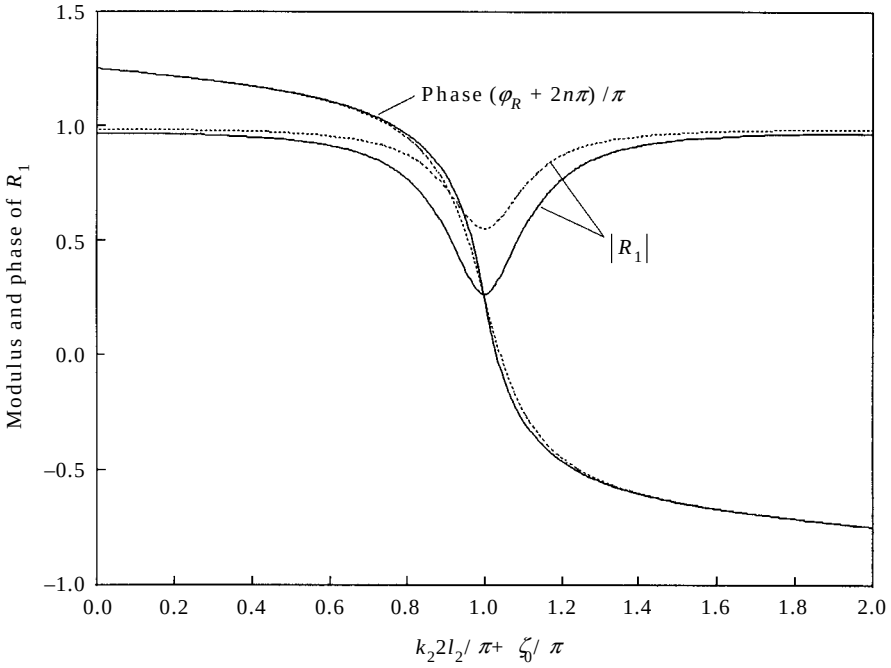

Figure 4. Modulus and phase of R_1 for a period of 2π in the case of a simple support at $x_2 = 0$ and with $|r_2| = 1$, $k_1 = k_2$ and $k_2 l_2 \eta/4$: ——, 0·1; – – –, 0·05. (ζ_0 is a phase shift, cf. equation (11a).)

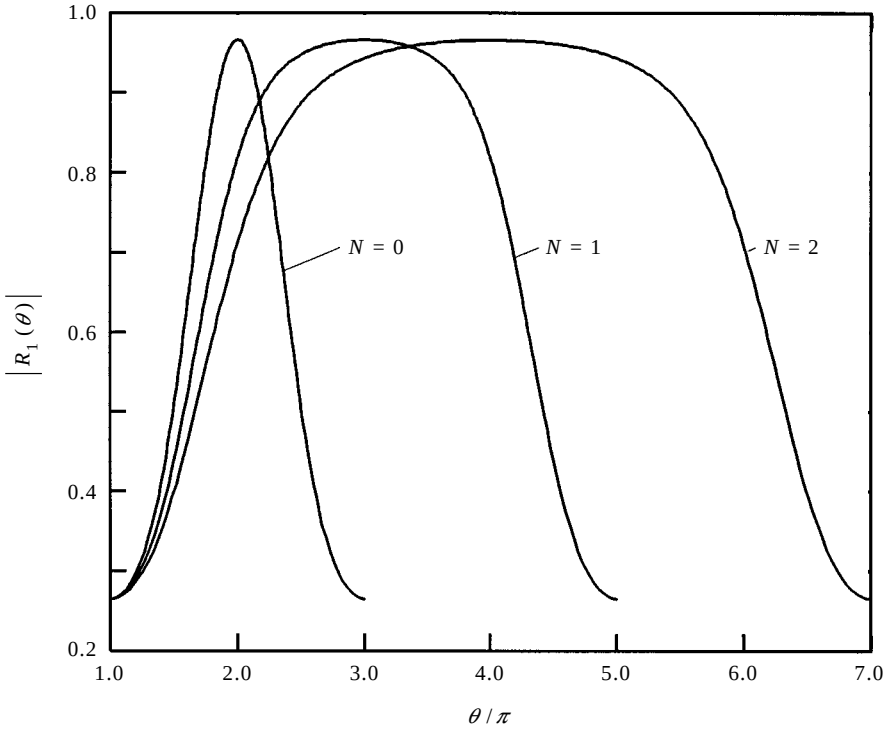

Figure 5. Modulus of R_1 versus phase θ for different values of $N = k_1 l_1/k_2 l_2$ with $k_2 l_2 \eta/4 = 0{\cdot}1$. The curve with $N = 0$ corresponds to $|R_1|$ versus phase of R_1 from Figure 4.

the phase θ as the independent variable and $|R_1(\theta)|$ as the dependent variable permits calculation of an average value, which will be denoted by $\langle|R_1|\rangle$: that is,

$$\langle|R_1|\rangle \equiv \langle|R_1 \, \mathrm{e}^{-\mathrm{j}k_1 2l_1}|\rangle, \tag{6}$$

where $\langle\,\rangle$ indicates average value. The value $\langle|R_1|\rangle$ expresses the average ratio of reflected to incident wave amplitude on the junction and indirectly the absorption of beam 2.

The average value $\langle|R_1|\rangle$ is seen to depend on the properties of the coupling given by its reflection and transmission coefficients and the two Helmholtz numbers ($k_1 l_1$ and $k_2 l_2$) of the beams. Intuitively, one would expect that the average ratio of reflected to incident wave amplitudes would depend of these parameters. Furthermore, the choice of θ as the independent variable also ties in with the principle of wave train closure. According to this principle, resonance occurs when the waves are reflected in phase; see reference [13], p. 206.

Having chosen θ as the independent variable and $|R_1 \exp(-\mathrm{j}k_1 2l_1)|$ as the dependent variable permits the mean of the ratio of reflected wave amplitude to incident wave amplitude to be calculated as

$$\langle|R_1|\rangle_{mean} = \frac{1}{\theta_2 - \theta_1} \int_{\theta_1}^{\theta_2} |R_1(\theta)| \, \mathrm{d}\theta, \tag{7}$$

where θ_1 and θ_2 are lower and upper integration limits. The determination of these two limits will be addressed in sections 3.1 and 3.2.

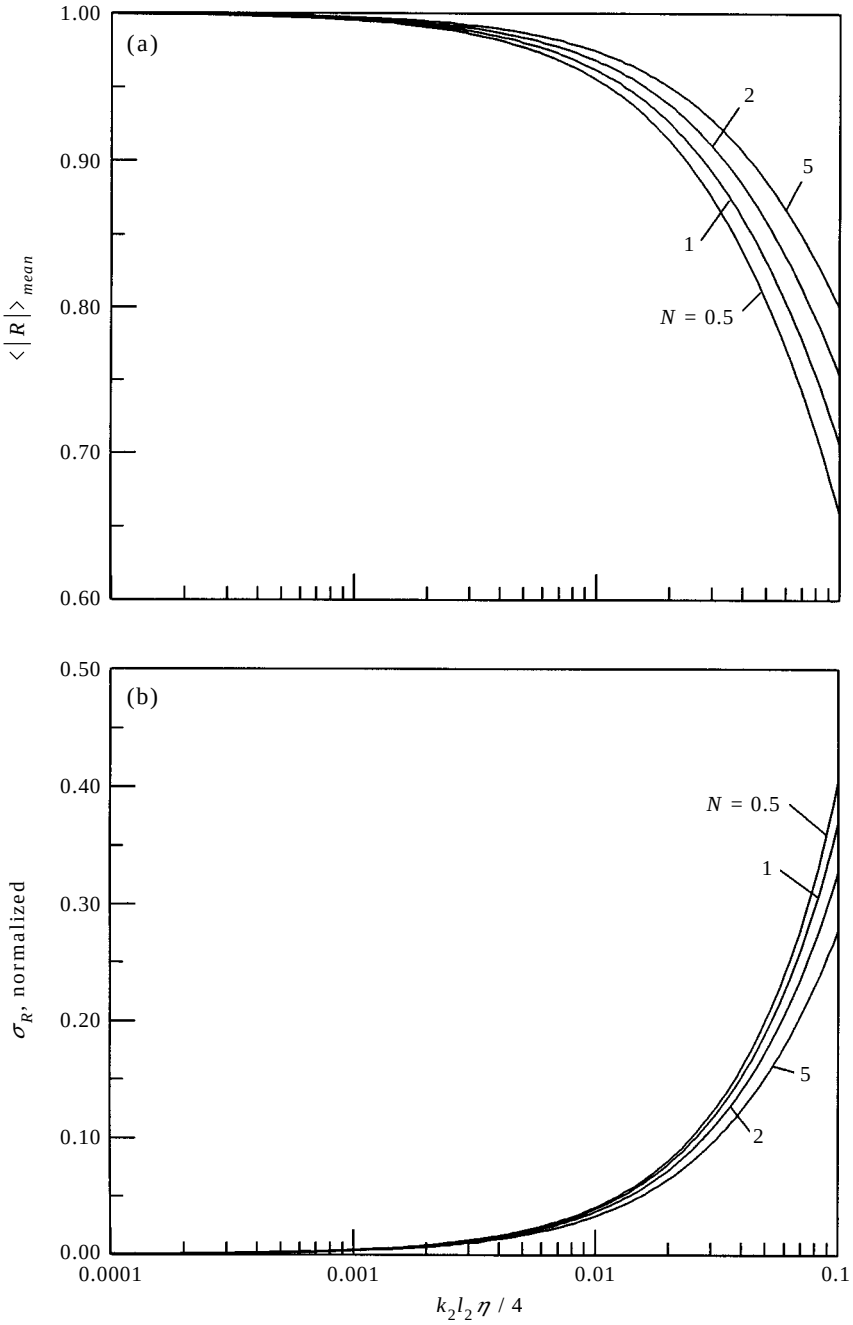

Figure 6. (a) The mean value of the net reflection $\langle |R_1| \rangle_{mean}$ and (b) the standard deviation σ_R for $|R_1|$ normalized with $\langle |R_1| \rangle_{mean}$ as a function of $k_2 l_2 \eta / 4$ for different values of N. Simple support with $k_1 = k_2$ and $|r_2| = 1$.

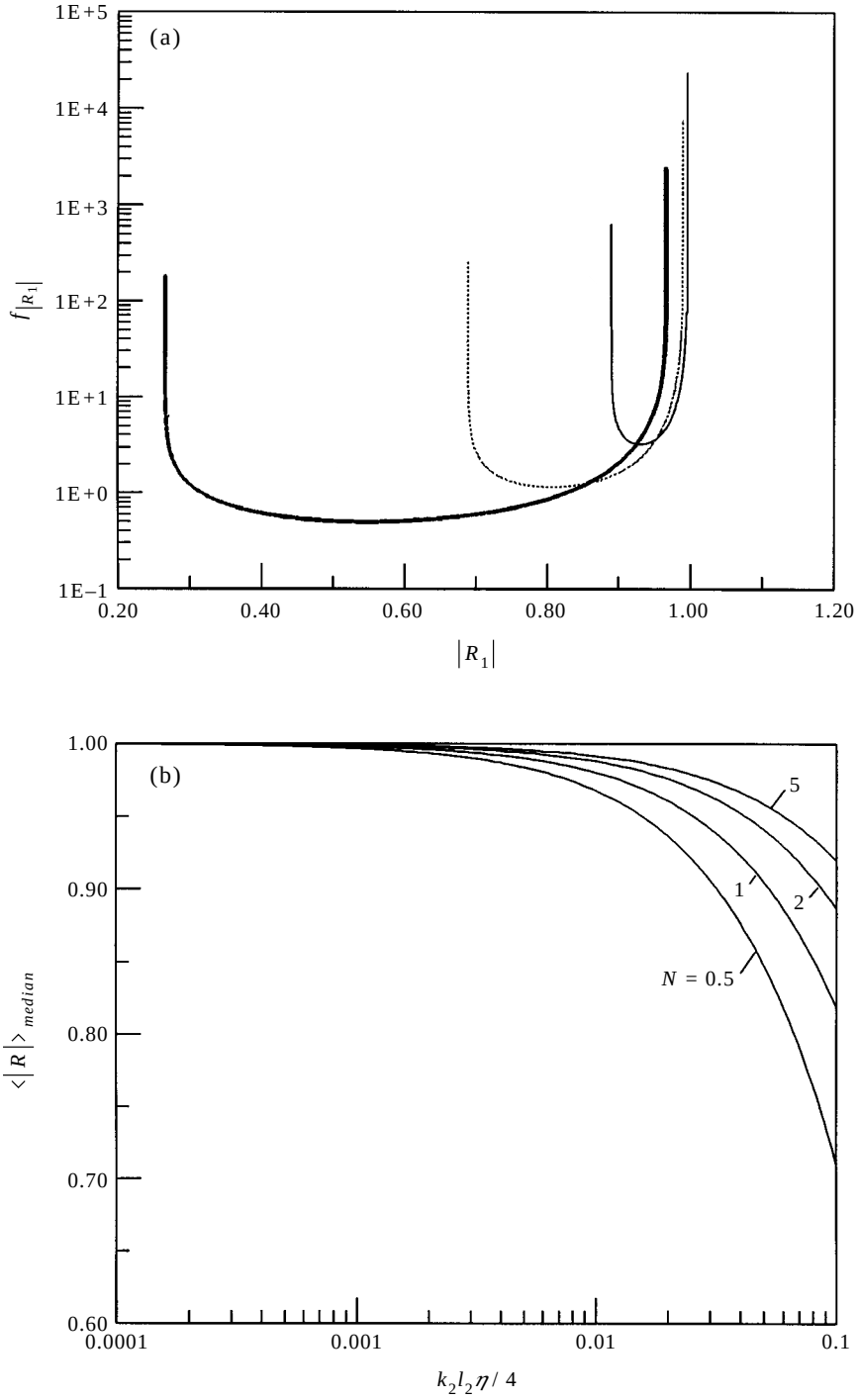

Figure 7. (a) Probability density function $f_{|R|}$ for $N = 2$ for $k_2 l_2 \eta/4 = 0{\cdot}1$ (——), $0{\cdot}0316$ (– – –), $0{\cdot}01$ (—); (b) $\langle |R_1| \rangle_{median}$ as a function of $k_2 l_2 \eta/4$ for different values of N. Simple support with $k_1 = k_2$ and $|r_2| = 1$.

3. NET REFLECTION

Before considering how the average value of value $R_1 \exp(-jk_1 2l_1)$, i.e., $\langle |R_1| \rangle$, should be calculated in practice, the general behaviour of the net reflection R_1 should briefly be considered.

The modulus of R_1 will be unity if there are no losses in beam 2. This situation corresponds to that when all incident power will eventually be reflected back. If on the other hand, energy is lost in beam 2, either because of dissipation in beam 2 and/or because power can pass through the right hand boundary of beam 2, then the modulus of R_1 will assume a value less than unity. This can be expressed as

$$|R_1| = 1 \text{ for } \eta_2 = 0 \wedge |r_2| = 1, \qquad |R_1| < 1 \text{ for } \eta_2 > 0 \vee |r_2| < 1, \tag{8a, b}$$

where η_2 is the damping loss factor for beam 2 and r_2 is the reflection coefficient at the right hand end of beam 2.

The net reflection R_1 can be regarded as a function of the parameter $k_2 2l_2$ of beam 2, in which the damping is expressed by the quantity $k_2 l_2 \eta/4$. If the damping in beam 2 varies only slightly with frequency then the net reflection R_1 can be considered as being a periodic function of $k_2 2l_2$ with the period 2π. In the following, the net reflection R_1 is assumed to have such a dependency and this greatly simplifies further analyses. It should be noted that a slowly varying loss factor is a limitation.

The Nyquist plot in Figure 3 illustrates the typical behaviour of the real and imaginary parts of the net reflection R_1 over a period of 2π for different values of $k_2 l_2 \eta/4$ and for a conservative termination at $x_2 = l_2$. All losses to beam 2 occur through dissipation in beam 2 as no energy is lost through its right end as $|r_2| = 1$. Figure 3 illustrates that the Nyquist plots of the net reflection R_1 are circles. When there are no losses in beam 2, i.e., $k_2 l_2 \eta/4 = 0$, then the radius of the circle will be unity and the centre of the circle will coincide with the origin (0, 0) of the co-ordinate system. As losses are introduced in beam 2, i.e., $k_2 l_2 \eta/4 > 0$, the radii of the circles will decrease and their centres will move away from the origin. As suggested in the previous section, the average value of $R_1 \exp(-jk_1 2l_1)$ should be determined by using θ as the independent variable. It is therefore important to notice how the damping in beam 2 influences the behaviour of the phase φ_R $(= \arg(R_1))$ and thereby $\arg(R_1 \exp(-jk_1 2l_1))$. For small values of $k_2 l_2 \eta/4$ the circle will enclose the origin and the phase of the net reflection R_1 will be unambiguous. As the damping in beam 2 increases the circles will no longer enclose the origin (0, 0) and the phase of R_1 will become ambiguous. For the example of the net reflection R_1 shown in Figure 3, this will occur only for the condition corresponding to $k_2 l_2 \eta/4 = 0{\cdot}2$.

As a consequence of this, the calculation of the average value $\langle |R_1| \rangle$ will be divided into two parts, that is to say the case characterized by the unambiguous phase and the case

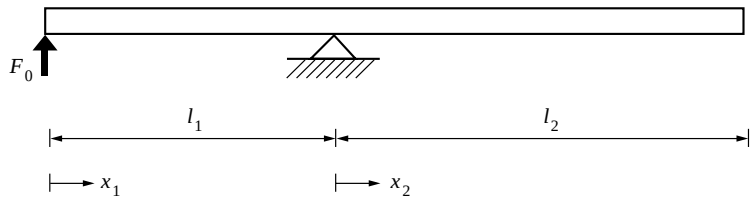

Figure 8. Two beams coupled via a simple support with $k_1 = k_2$ and $\eta_1 = \eta_2$. The free end of the left beam is driven by a harmonic point force F_0.

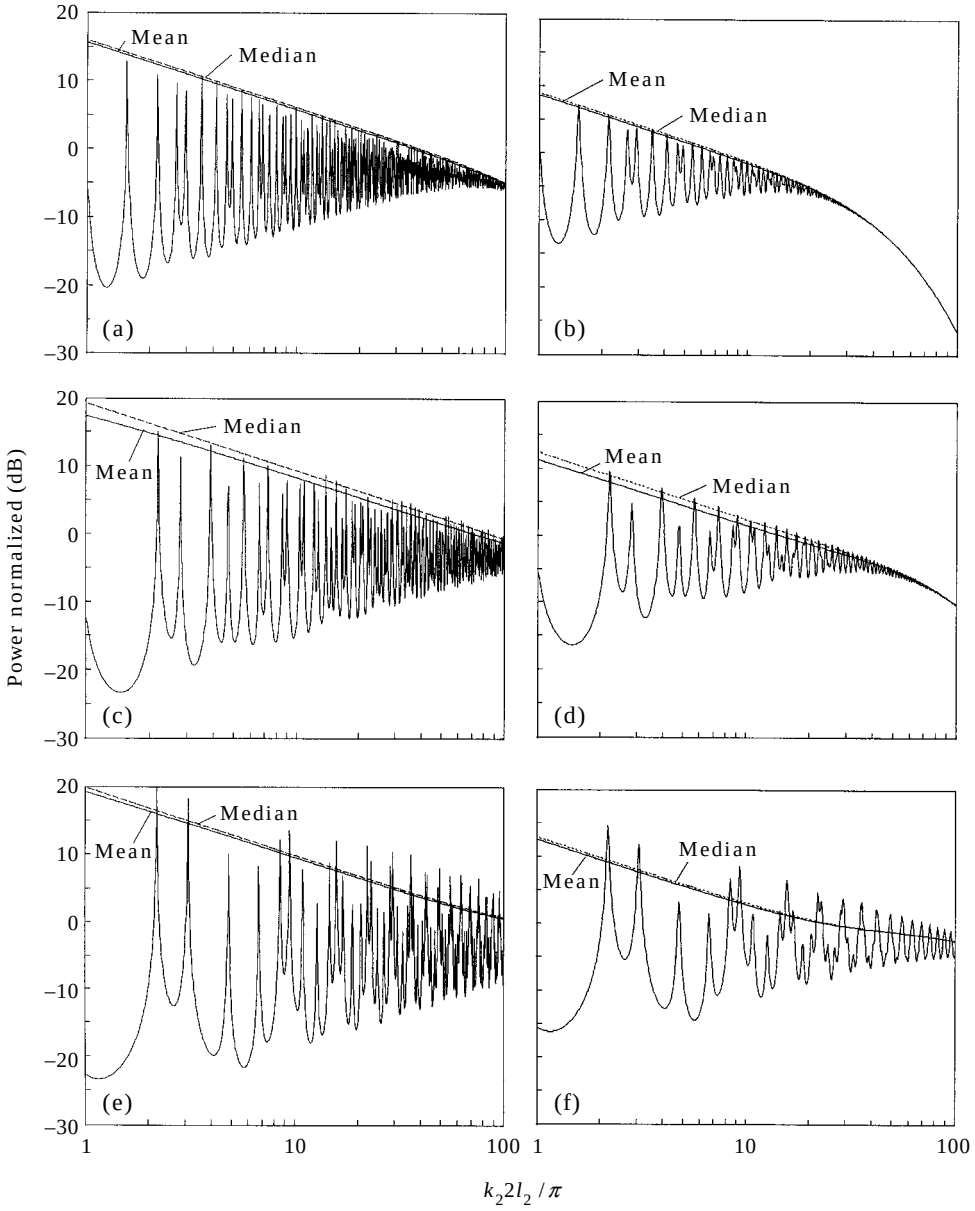

Figure 9. Comparison between exact and estimated maximum levels of transmitted power at the middle of the driven beam for Helmholtz ratio $N = 3{\cdot}1$ (a, b), $1{\cdot}2$ (c, d), $0{\cdot}3$ (e, f). Two beams coupled via simple support with $\eta = 0{\cdot}01$ (a, c, e) and $0{\cdot}05$ (b, d, f), $k_1 = k_2$, $|r_2| = 1$ and $x_1 = l_1/2$.

characterized by an ambiguous phase. From the Nyquist plots it can be shown that the phase of the net reflection R_1 will be unambiguous when the condition

$$|r_{12}| \leqslant |t_{12}t_{21}r_2|/(e^{k_2 l_2 \eta/2} - |r_{21}r_2|) \tag{9}$$

is fulfilled.

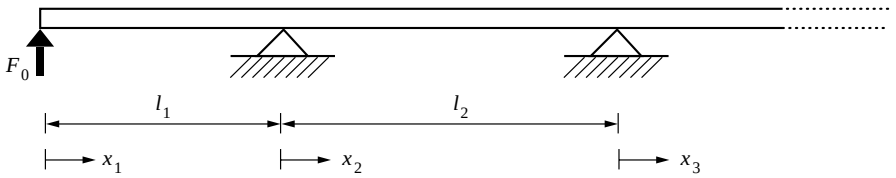

Figure 10. System consisting of two finite beams coupled via a simple support and terminated by another simple support and a semi-infinite beam; $k_1 = k_2 = k_3$ and $\eta_1 = \eta_2 = \eta_3$.

Of interest are also the maximum and minimum values of $|R_1|$. These simply correspond to the vector positions which are furthest away from and closest to the origin. These values can be determined as

$$|R_1|_{max} = |r_{12}| + \frac{|t_{12}t_{21}r_2|}{e^{k_2 l_2 \eta/2} + |r_{21}r_2|}, \qquad |R_1|_{min} = \left| \frac{|t_{12}t_{21}r_2|}{e^{k_2 l_2 \eta/2} - |r_{21}r_2|} - |r_{12}| \right|. \tag{10a, b}$$

If the phase of r_2 is denoted by φ_2 and the phase of r_{21} is denoted by φ_{21} then $|R_1|_{max}$ and $|R_1|_{min}$ will occur when

$$k_2 2l_{2\,max} = \varphi_{21} + \varphi_2 + (2n-1)\pi, \qquad n = 0, 1, 2, 3, \ldots, \tag{11a}$$

$$k_2 2l_{2\,min} = \varphi_{21} + \varphi_2 + 2n\pi, \qquad n = 0, 1, 2, 3, \ldots, \tag{11b}$$

where n is an integer.

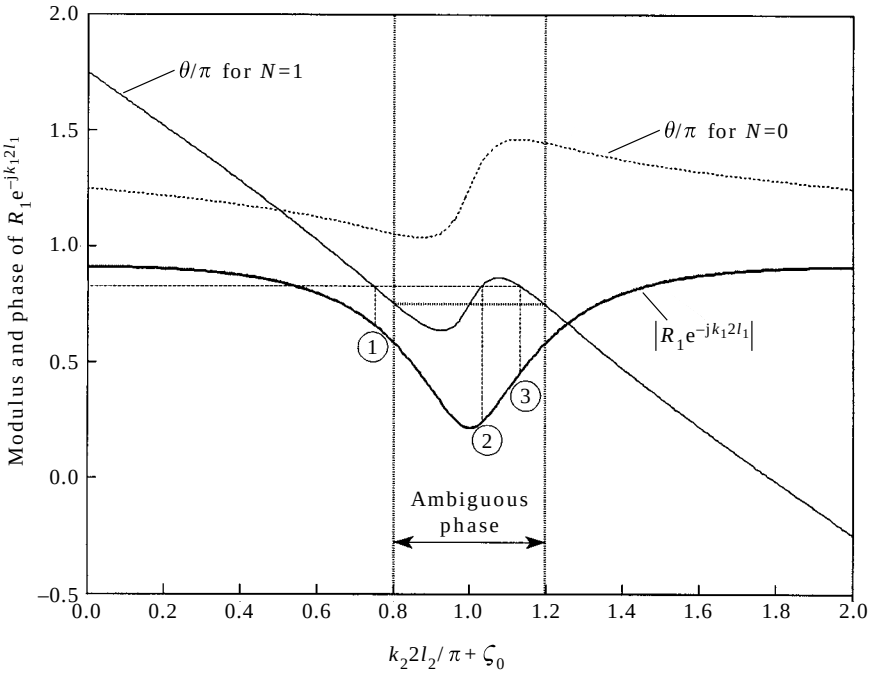

Figure 11. Modulus and phase of $R_1 \exp(-jk_1 2l_1)$ for two different values of $N = k_1 l_1 / k_2 l_2$. The system consists of two finite beams and a semi-infinite beam coupled via simple supports and with $k_1 = k_2 = k_3$ and $k_2 l_2 \eta / 4 = 0{\cdot}1$. ($\zeta_0$ is a phase shift, cf. equation (11a).)

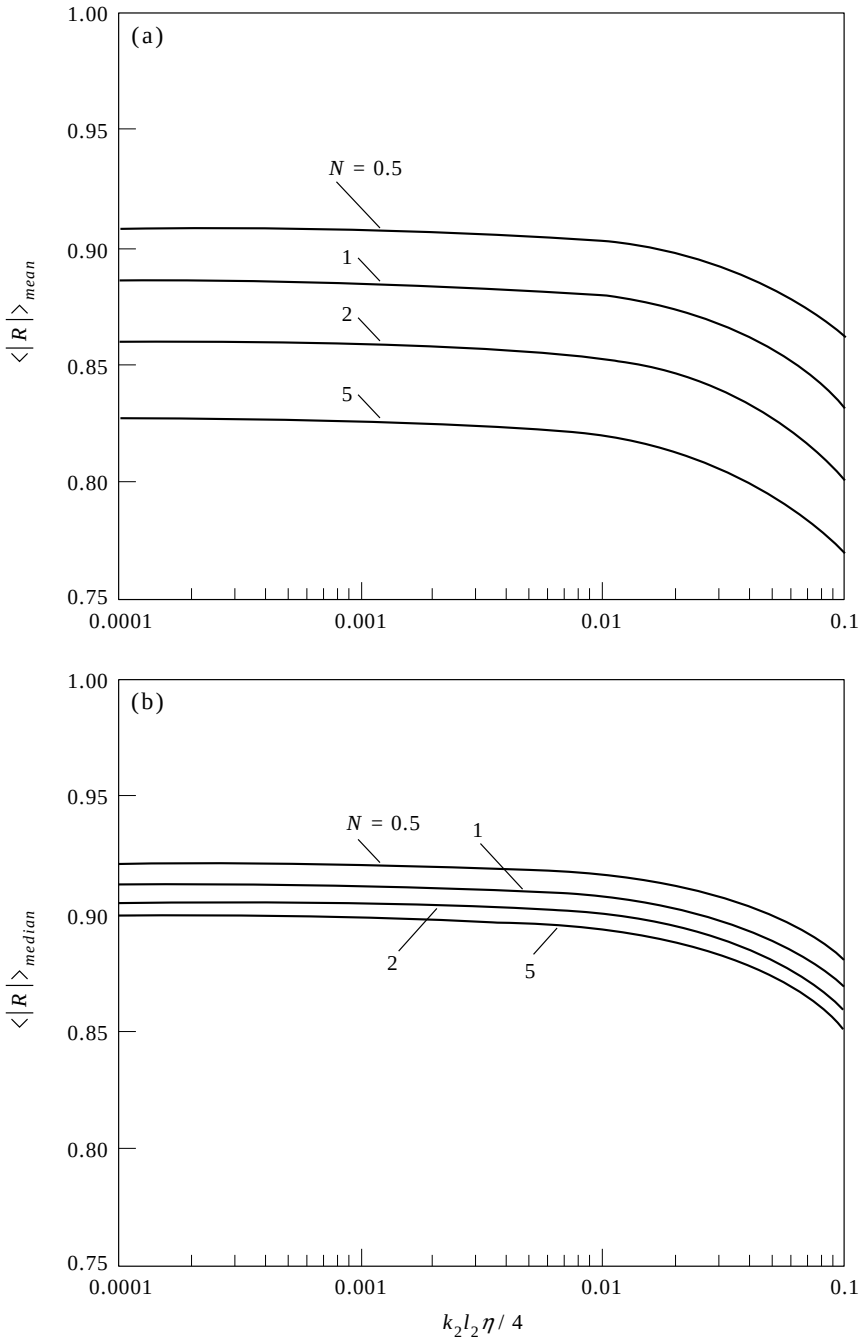

Figure 12. (a) $\langle |R_1| \rangle_{mean}$ and (b) $\langle |R_1| \rangle_{median}$ as a function of $k_2 l_2 \eta/4$ for different Helmholtz ratios $N = k_1 l_1 / k_2 l_2$. System as depicted in Figure 10 with simple supports and $k_1 = k_2 = k_3$.

3.1. UNAMBIGUOUS PHASE

Figure 4 shows the typical behaviour of the modulus and phase of the net reflection R_1 when the phase is unambiguous. As mentioned above, when no energy is lost through the end of the second beam ($|r_2| = 1$) and there is no dissipation in the second beam ($\eta_2 = 0$),

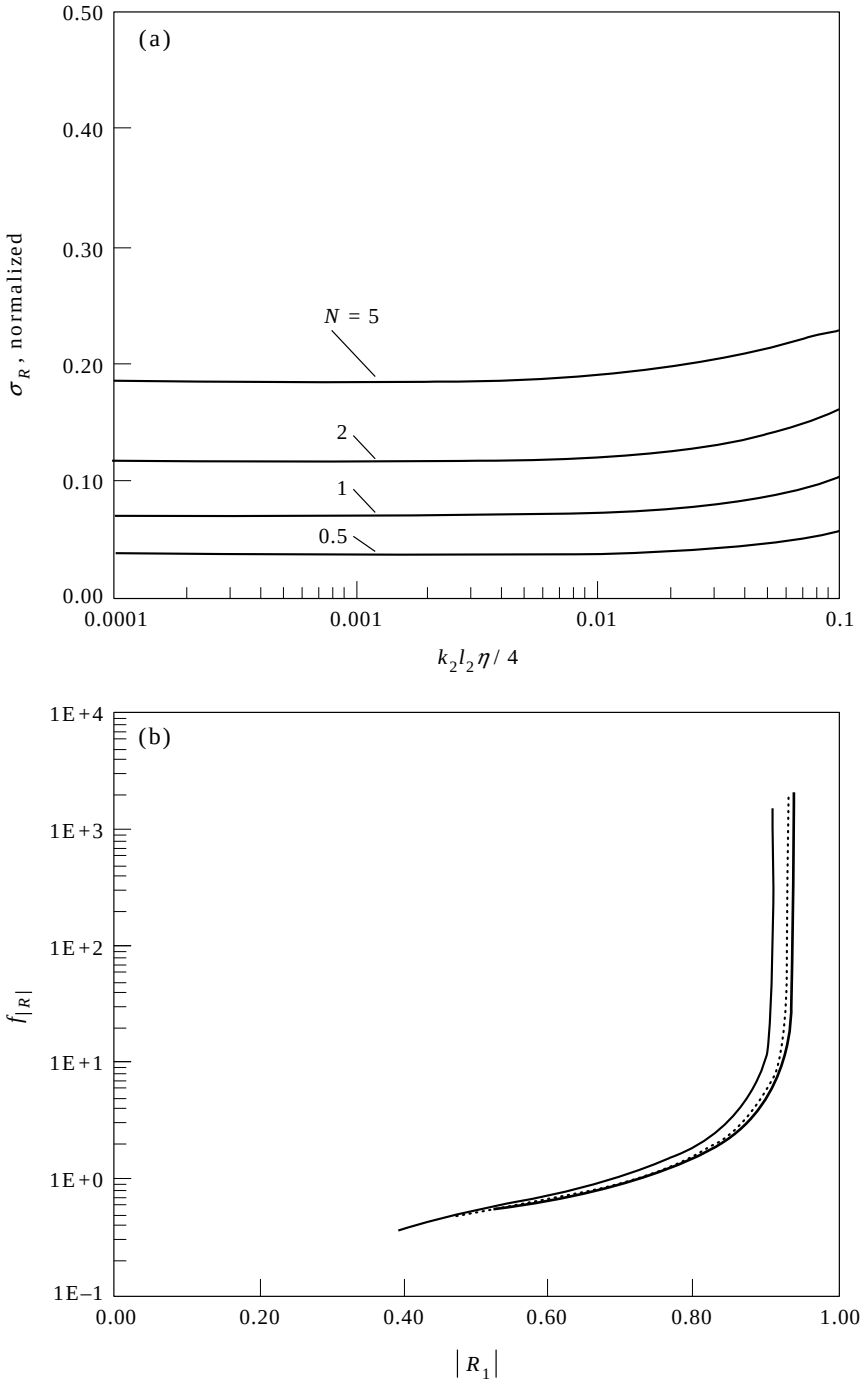

Figure 13. (a) Standard deviation σ_R normalized with $\langle |R_1| \rangle_{mean}$ as a function of $k_2 l_2 \eta/4$ for different Helmholtz ratios $N = k_1 l_1 / k_2 l_2$. (b) Probability density function $f_{|R|}$ for $N = 2$ for $k_2 l_2 \eta/4 = 0{\cdot}1$ (——), $0{\cdot}0316$ (– – –),$0{\cdot}01$ (—). Both for a system as depicted in Figure 10 with simple supports and $k_1 = k_2 = k_3$.

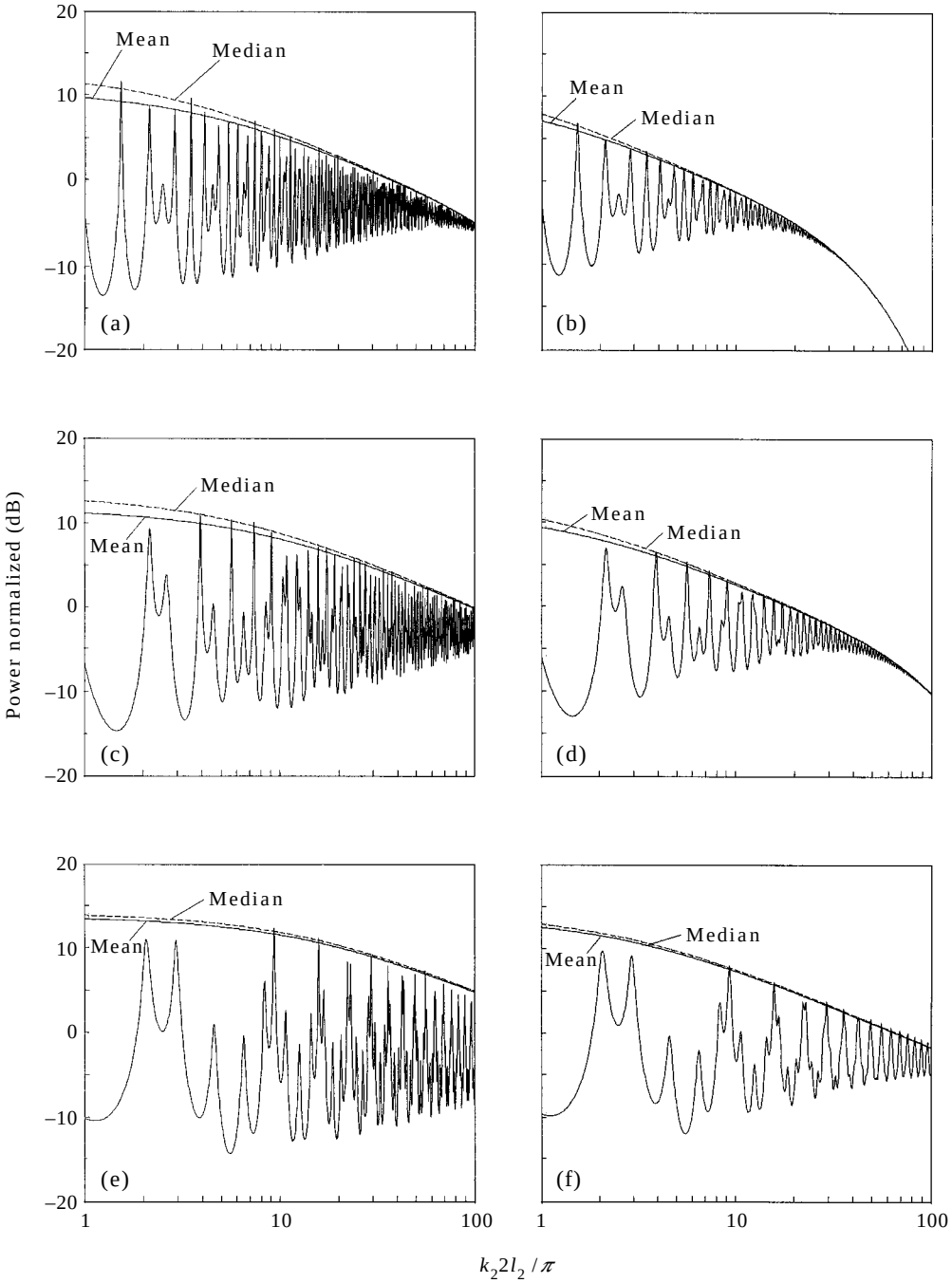

Figure 14. Comparisons between exact and estimated maximum levels of transmitted power at the middle of the driven beam for Helmholtz ratio $N = 3{\cdot}1$ (a, b), $1{\cdot}2$ (c, d), $0{\cdot}3$ (e, f). Two beams and a semi-infinite beam coupled via simple supports with $\eta = 0{\cdot}01$ (a, c, e) and $0{\cdot}05$ (b, d, f), $k_1 = k_2 = k_3$ and $x_1 = l_1/2$.

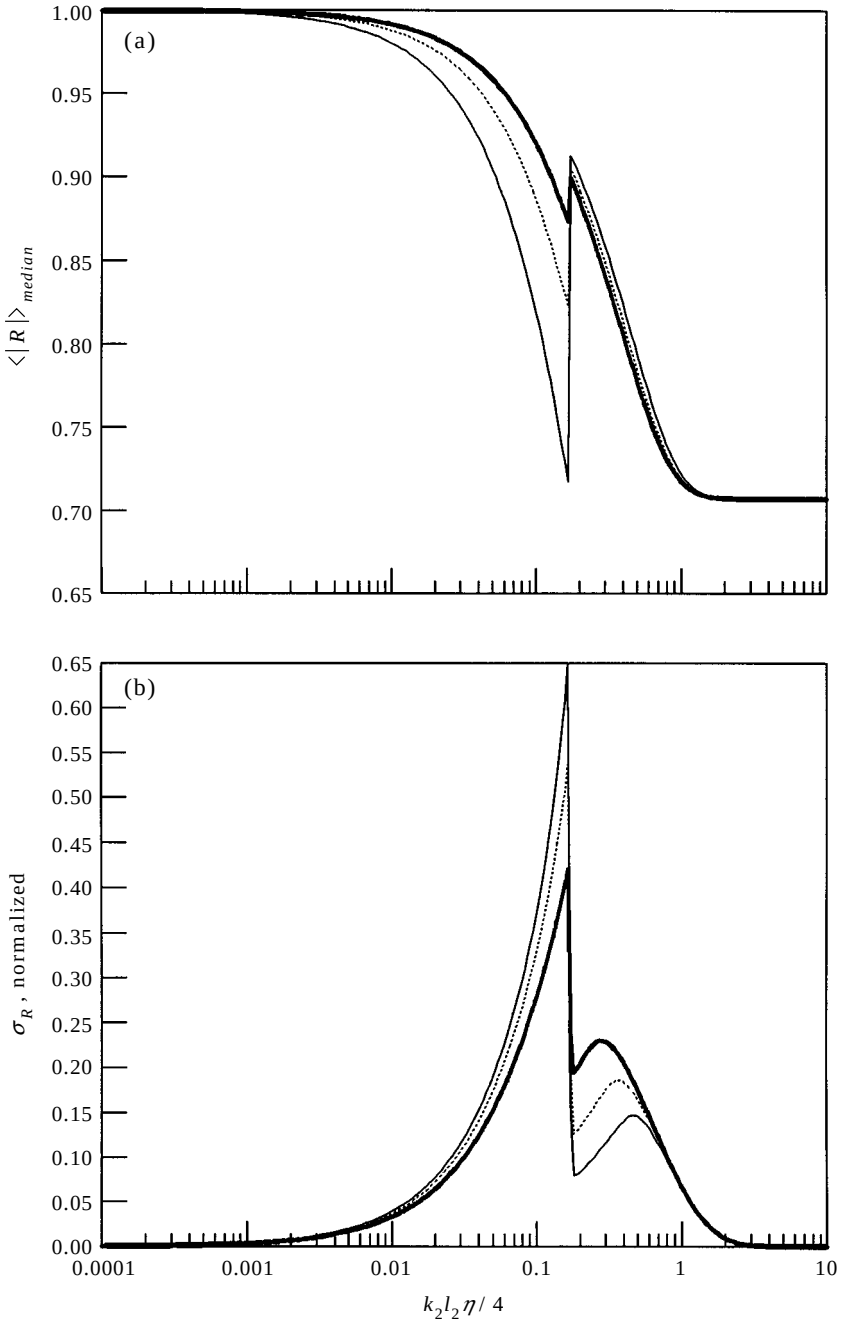

Figure 15. General behaviour of (a) $\langle |R_1| \rangle_{median}$ and (b) the normalized standard deviation σ_R as a function of $k_2 l_2 \eta/4$ for different values of Helmholtz ratio $N = k_1 l_1 / k_2 l_2$ for a system coupled via a simple support and with $k_1 = k_2$. ——, $N = 1$; – – –, $N = 2$; ═══, $N = 5$.

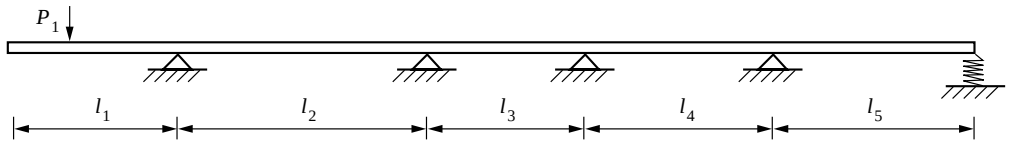

Figure 16. System of five beams with identical wave numbers k coupled via simple supports. Dimensions: (lengths) $l_1 = 0{\cdot}3$ m, $l_2 = 0{\cdot}25$ m, $l_3 = 0{\cdot}35$ m, $l_4 = 0{\cdot}2$ m, $l_5 = 0{\cdot}4$ m, (width) $b = 0{\cdot}04$ and (height) $h = 0{\cdot}01$ m. Material brass. The first beam is free at the end while the fifth beam is supported by a damped spring with a stiffness of $s = 20(1 + \mathrm{j}0{\cdot}1)$ N/m. A vibrational power P_1 is injected into the first beam.

then the modulus of the net reflection R_1 will be unity corresponding to the case where all the energy incident on the joint will eventually be reflected back. When energy is dissipated in the second beam, $|R_1|$ will assume values less than unity. However, the effect of this dissipation is not uniformly distributed over a period of $k_2 2l_2$. A notch will appear in the modulus of R_1 corresponding to the region in the frequency domain which has the highest dissipation. If the damping is increased it will mainly be noticeable by an increase in depth of the notch.

The importance of this notch is far more significant than a first glance might suggest. The reason is that the large phase shift of R_1 coincides with the notch. This relation is illustrated in Figure 5 which shows $|R_1(\theta)|$ versus the phase θ for different values of N. Of course the case for $N = 0$ cannot exist in practice, but it is included here because it illustrates $|R_1|$ versus the phase φ_R from Figure 4. As N is increased the phase of $\exp(-\mathrm{j}k_1 2l_1)$ is added to φ_R. Thus, the case for $N > 0$ corresponds to "stretched translation" of $N = 0$, but with the different parts being stretched to various degrees. From Figure 5, the influence of the notch on $\langle |R_1| \rangle$ is seen to decrease with increasing values of the Helmholtz ratio N. Because of the symmetry only half of a period of R_1 needs to be considered when calculating $\langle |R_1| \rangle$. The independent variable, θ, is assumed to have a uniform probability density in the range corresponding to half a period, that is, $\theta \in [\zeta_0; \zeta_0 + \pi(N + 1)]$, where $\zeta_0 = k_2 2l_{2\,max}$ cf. (equation 11a). The mean of the net reflection $\langle |R_1| \rangle$ can then be calculated as

$$\langle |R_1| \rangle_{mean} = \frac{1}{\pi(N+1)} \int_{\zeta_0}^{\zeta_0 + \pi(N+1)} |R_1(\theta)| \, \mathrm{d}\theta, \tag{12}$$

and the standard deviation of the net reflection σ_R can be calculated from

$$\sigma_R^2 = \frac{1}{\pi(N+1)} \int_{\zeta_0}^{\zeta_0 + \pi(N+1)} \{|R_1(\theta)| - \langle |R_1| \rangle_{mean}\}^2 \, \mathrm{d}\theta. \tag{13}$$

It should be noted that the thereby calculated mean of the net reflection $\langle |R_1| \rangle$ and its corresponding standard deviation σ_R are independent of the exact boundary conditions of

TABLE 1

Calculated coupling loss factors η_{pq} and η_{qp} for the system shown in Figure 16

p to q	N	D_N (median)	η_{pq}/η_q	η_{qp}/η_p
1 to 2	1·20	1·7284	5·30	6·36
3 to 2	1·40	1·5365	2·37	3·31
3 to 4	1·75	1·3157	1·10	1·92
5 to 4	2·00	1·2117	0·77	1·53

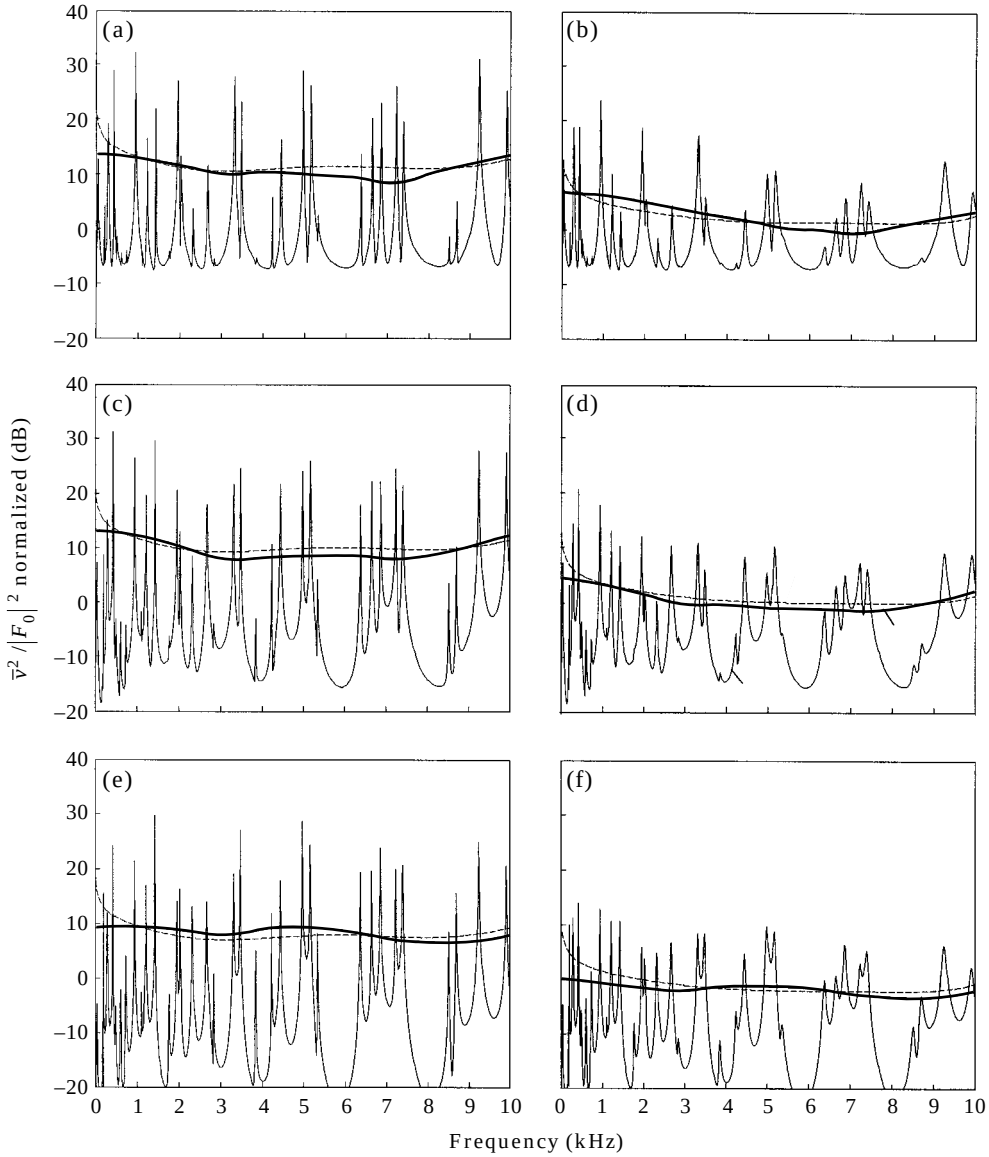

Figure 17. Mean square velocities normalized with $(m'c_B)^{-2}$ for the first three beams of the five-beam system shown in Figure 16 for two different values of the loss factor $\eta = 0{\cdot}001$ (a, c, e) and $\eta = 0{\cdot}01$ (b, d, f). ——, Exact solution; —, exact solution averaged; – – –, present method. (a) and (b) Beam 1, (c) and (d) Beam 2, (e) and (f) Beam 3.

beam 1 at $x_1 = 0$ and of beam 2 at $x_2 = l_2$. To be more precise, they are independent of the phases of r_0 and r_2. Thus, $\langle |R_1| \rangle$ is the same for different combinations of boundary conditions of these two ends (e.g., free, simply supported, sliding etc.) for which $|r_0|$ and $|r_2|$ are identical. For r_0 this is easy to see as r_0 is not involved in the averging process. To

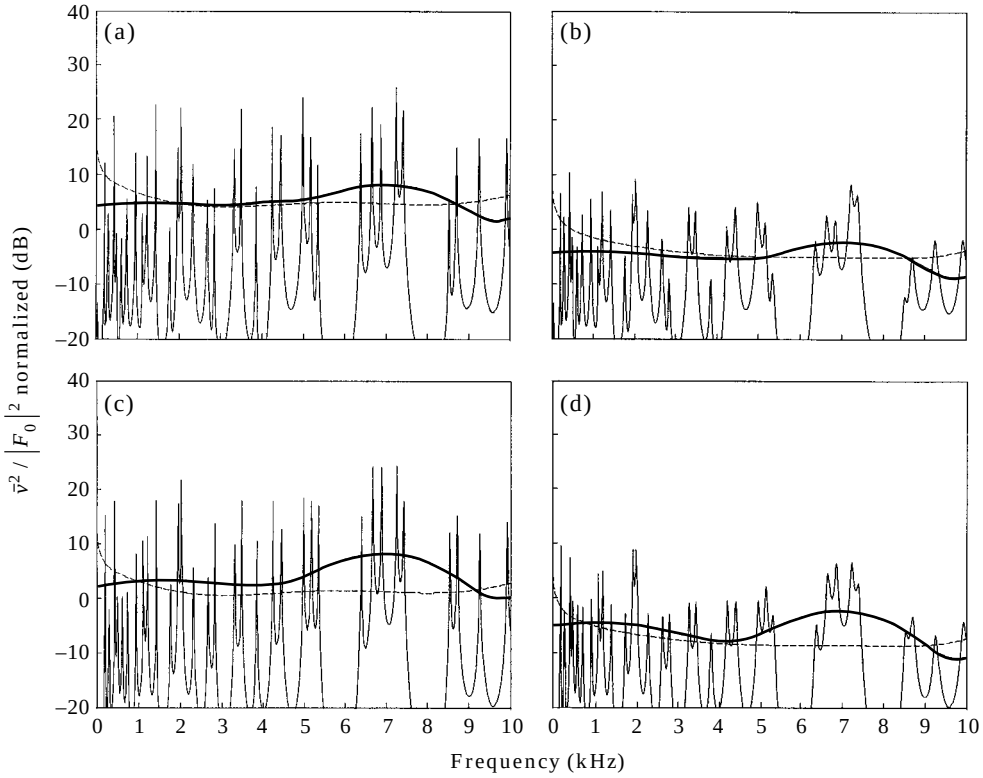

Figure 18. Mean square velocities normalized with $(m'c_B)^{-2}$ for the last two beams of the five-beam system shown in Figure 16 for two different values of the loss factor $\eta = 0{\cdot}001$ (a, c) and $\eta = 0{\cdot}01$ (b, d). ——, Exact solution; —, exact solution averaged; ——, present method. (a) and (b) Beam 4, (c) and (d) Beam 5.

realize that the same applies for r_2 might be a little subtle. From equation (11) it can be seen that the phase of r_2 determines the location of the notch. However, since the general behaviour of the modulus and phase of the net reflection R_1 is independent of the actual location of the notch, the values calculated from equations (12) and (13) will be equally valid for all types of boundary conditions for which the modulus of r_2 are identical.

Despite the fact that the expression for the net reflection R_1 is relatively simple, it is not easy to give an analytical expression for $\langle |R_1| \rangle$ as this will be rather complicated. However, it is quite straightforward to calculate numerically $\langle |R_1| \rangle$ and σ_R as functions of $k_2 l_2 \eta / 4$

TABLE 2

Comparison of coupling loss factors at 5 kHz

p to q	η_{pq} Improved	η_{pq} Equation (18)	η_{pq} Mace [20]
1 to 2	$5{\cdot}3 \times 10^{-3}$	29×10^{-3}	$0{\cdot}21 \times 10^{-3}$
3 to 2	$2{\cdot}4 \times 10^{-3}$	25×10^{-3}	$0{\cdot}19 \times 10^{-3}$
3 to 4	$1{\cdot}8 \times 10^{-3}$	25×10^{-3}	$0{\cdot}16 \times 10^{-3}$
5 to 4	$0{\cdot}8 \times 10^{-3}$	22×10^{-3}	$0{\cdot}14 \times 10^{-3}$

for different values of the Helmholtz ratio N. The results of such calculations are shown in Figure 6 for a range of typical values of N.

From Figures 6(a) it can be seen that $\langle|R_1|\rangle$ assumes its greatest values when N is large and that it decreases with decreasing values of N. The mean of the net reflection $\langle|R_1|\rangle$ can be thought of as a measure of the dissipation in the second beam. Thus, a large value of $\langle|R_1|\rangle$ corresponds to a small dissipation in the second beam and vice versa. Thus, it can be seen from Figure 6(a) that the energy dissipation in the receiving beam will be largest, as expected, when the receiving beam is relatively long as compared to the source beam.

Figure 6(b) shows the corresponding normalized standard deviation σ_R. The standard deviation σ_R increases at low modal overlap when the losses in the second beam increase. The obvious reason is that the notch of the modulus of the net reflection R_1 becomes more profound for increasing values of $k_2 l_2 \eta/4$. As the influence of the notch is more notable for small ratios of N these cases will have the highest standard deviation. Evidently, the net reflection is related only indirectly to the net transmitted power through equations (1) and (4). Nevertheless, since the standard deviation σ_R increases with $k_2 l_2 \eta/4$, which is proportional to the square root of frequency, then one would expect greater fluctuations in the power transmission as frequency is increased. Investigations into the net power transmission in coupled systems ae described in [15]. Contrary to the expectations of the authors the fluctuations of the transmitted power did not seem to decrease with increasing frequency. The increase of the standard deviation σ_R with $k_2 l_2 \eta/4$ could be a possible explanation for this phenomenon.

A typical example of the probability density function $f_{|R|}$ of the net reflection R_1 for a system with $N = 2$ is shown in Figure 7(a) for different values of $k_2 l_2 \eta/4$. Normally, for a bell-shaped probability density functions, like the normal distribution, the mean would be a good estimate of the expected value because the mean is the value that minimizes the quantity $\int |R_1(\theta) - \langle|R_1|\rangle|^2 \, \mathrm{d}\theta$. However, for the present case the probability density function $f_{|R|}$ is not symmetric and has furthermore two large tails corresponding to $|R_1|_{max}$ and $|R_1|_{min}$, respectively. Because of the behaviour of the probability density function, the mean is a less appropriate estimate of the expected value. A more correct estimate of the expected value would be anticipated by employing the median. The median minimizes the quantity $\int |R_1(\theta) - \langle|R_1|\rangle| \, \mathrm{d}\theta$ and corresponds to 50% of the cumulative probability function. The median of the net reflection $\langle|R_1|\rangle_{median}$ is shown in Figure 7(b), and it is seen to assume values that are slightly higher than those for the mean $\langle|R_1|\rangle_{mean}$.

Later on when employing the numerically calculated values of $\langle|R_1|\rangle_{mean}$ and $\langle|R_1|\rangle_{median}$ it will be convenient to utilize the fact that these values have an excellent fit with functions of the type

$$\langle|R_1|\rangle \approx \exp(-D_N k_2 l_2 \eta_2/2), \tag{14}$$

where D_N is a constant which depends on the value of the Helmholtz ratio N and the transmission efficiency τ of the coupling.

3.1.1. *Numerical example*

The calculation of $\langle|R_1|\rangle$ relies on numerical integration and some sort of verification would therefore be desirable. This example tends to do so by using the calculated value of $\langle|R_1|\rangle$ to predict the maximum levels of transmitted power in beam 1 and draws comparisons with exact calculations. The system considered (see Figure 8) consists of two finite beams with $k_1 = k_2$ coupled via a simple support. The first beam is driven at its free end by a harmonic point force and beam 2 is also free at its far end $x_2 = l_2$.

For this system the net transmitted power in beam 1 will be given by equation (4). Based on this equation, the approximate maximum levels of net transmitted power can be found as

$$P_{1,\max}(x_1) \approx \frac{|F_0|^2}{2m_1' c_{B_1}} \frac{e^{-k_1 x_1 \eta/2} - \langle |R_1| \rangle^2 e^{-k_1(2l_1 - x_1)\eta/2}}{[1 - \langle |R_1| \rangle e^{-k_1 l_1 \eta/2}]^2}, \tag{15}$$

where all the phases in equation (4) have been omitted. Equation (15) is, of course, a crude approximation but since $\langle |R_1| \rangle$ is based on information about the coupling and the two Helmholz numbers, it gives good estimates of the maximum levels.

This is demonstrated by the results shown in Figure 9 which shows comparisons between exact and approximate calculations of the net transmitted power in the middle of the first beam. The exact results are calculated from equation (4), and the corresponding estimated maximum values were calculated by using equation (15), with $\langle |R_1| \rangle$ being expressed in turn by $\langle |R_1| \rangle_{mean}$ and $\langle |R_1| \rangle_{median}$. These calculations were carried out for different values of N and for two values of the loss factor $\eta = 0{\cdot}01$ and $0{\cdot}05$.

The predicted maximum values are found to be in excellent agreement with the exact values for values of the Helmholtz ratio $N \geqslant 1$. However, for $N < 1$ the agreement is less good because of the frequency modulation of the peaks in the net transmitted power. This modulation is caused by the variation of $|R_1|$ with frequency, cf. Figure 4. This can be explained as follows. The phase of R_1 evolves during half a period to π. That N is less than 1 means that the factor $k_1 2l_2$ will add a contribution to the phase θ that is less than π. The consequence is that the net transmitted power will be modulated in frequency as shown in Figure 9 for $N = 0{\cdot}3$. For the case of $N \geqslant 1$ the total evolved phase will be equal to or greater than 2π. Consequently, at least one resonance will occur during half a period of R_1 and the net transmitted power will therefore not be modulated in frequency. Thus, the calculated value of $\langle |R_1| \rangle$ is only accurate when the condition

$$N = k_1 l_1 / k_2 l_2 \geqslant 1, \tag{16}$$

is fulfilled.

It is furthermore noticed that the predicted maximum values determined with $\langle |R_1| \rangle_{median}$ are slightly more accurate than those obtained by using $\langle |R_1| \rangle_{mean}$.

3.2. AMBIGUOUS PHASE

When the circles of the Nyquist plot do not enclose the origin as in Figure 3 for $k_2 l_2 \eta / 4 = 0{\cdot}2$, then the phase of R_1 will become ambiguous. The cause can either be a high dissipation in beam 2 and/or that power can be lost through the end of beam 2 at $x_2 = l_2$, i.e., $|r_2| < 1$ as depicted in Figure 10. The latter case is the one that will be used to illustrate the calculation of $\langle |R_1| \rangle$ when the phase is ambiguous.

The first and second elements of the system are similar to those in the case previously examined with the unambiguous phase except that the end of the second beam is no longer free but is connected to a semi-infinite beam via a simple support. The modulus and phase of $R_1 \exp(-\mathrm{j} k_1 2l_1)$ for this system are shown in Figure 11. The shape of the modulus of R_1 is seen to resemble that of R_1 in Figure 4. The behaviour of the phase θ is shown for two values of the Helmholtz ratio: $N = 0$ and $N = 1$. The case of practical interest is when $N > 0$.

The ambiguity of the phase is illustrated in Figure 11. To the value of the phase $\theta/\pi \approx 0{\cdot}8$ there are seen to correspond not less than three values of $|R_1 \exp(-\mathrm{j} k_1 2l_1)|$, indicated by the encircled numbers: 1, 2 and 3. Because the denominators of

equations (1) and (4) are dominating it can be seen that the value of 1 will result in a higher level of transmitted power than the levels of 2 and 3. This might seem somewhat surprising as the values of 2 and 3 correspond to higher absorptions. This ambiguity in the phase could, of course, be ignored by simply numerically integrating over the whole period. However, if the resulting values of $\langle|R_1|\rangle$ were to be verified with the use of equations (4) and (15) one would find that the predicted maximum values were far too low. The reason is that to 2 and 3 correspond maximum levels of the transmitted power which are insignificant in comparison with the value related to 1. Therefore, the best way to handle this ambiguity of the phase is to exclude the ambiguous part of the phase θ and to integrate the remaining part.

The ambiguous zone is shown in Figure 11 as the region between the two vertical dotted lines. This zone is determined in the following manner. First, the phase value θ_{middle} at the middle of the period is determined. In Figure 11 θ_{middle} is found at the position $(k_2 2l_2 + \zeta_0)/\pi = 1{\cdot}0$. Second, the value of $(k_2 2l_2 + \zeta_0)/\pi$ is decreased until the phase θ is equal to θ_{middle}; this gives the lower bound of the ambiguous zone which in Figure 11 corresponds to $(k_2 2l_2 + \zeta_0)/\pi \approx 0{\cdot}8$. Third, by starting again from the middle of the period, $(k_2 2l_2 + \zeta_0)/\pi$ is increased until the phase θ is equal to θ_{middle}. This gives the upper bound of the ambiguous zone which in Figure 11 coresonds to the value $(k_2 2l_2 + \zeta_0/\pi) \approx 1{\cdot}2$.

For the calculation of the mean, the standard deviation, the median and the probability density function it is sufficient to consider only half a period. Figures 12 and 13 show these statistical descriptors for the system shown in Figures 10 as a function of $k_2 l_2 \eta/4$ and for different values of the Helmholtz ratio N. Here it can be seen that the asymptotic values of $\langle|R_1|\rangle_{mean}$ and $\langle|R_1|\rangle_{median}$ are no longer unity for $k_2 l_2 \eta/4$ tending towards zero, because of the energy lost to the semi-infinite beam. Furthermore, and in contrast to a system with unambiguous phase, the highest values of $\langle|R_1|\rangle$ are found to occur for small values of N. Thus, the maximum levels of transmitted power will be lowest if the driven beam is long and highest when it is short.

Figure 13(a) shows the normalized standard deviation in the case of ambiguous phase and it is seen that the normalized standard deviation increases with the losses in the second beam and that it is highest for large values of N. Figure 13(b) shows the probability density function which evidently is not symmetric, as it exhibits a large tail. The median will therefore also in this case be a better estimate of the expected value.

Also in this case it is convenient to utilize the fact that the numerically calculated values of $\langle|R_1|\rangle_{mean}$ and $\langle|R_1|\rangle_{median}$ for the ambiguous phase have an excellent fit with functions of the type

$$\langle|R_1|\rangle \approx C_N \exp(-D_N k_2 l_2 \eta_2/2), \qquad C_N < 1, \tag{17}$$

where C_N and D_N are constants that depend on the value of the Helmholtz ratio N, the transmission efficiency τ of the coupling and r_2. From Figure 13 it can be seen that C_N assumes values less than unity.

3.2.1. *Numerical example*

In order to verify the calculated values of $\langle|R_1|\rangle_{mean}$ and $\langle|R_1|\rangle_{median}$, these were substituted in equation (14) and compared with equation (4). The system examined is depicted in Figure 10: that is, two finite beams and a semi-infinite beam connected via simple supports and with $k_1 = k_2 = k_3$. Figure 14 shows the comparisons between predicted maximum values and the exact values. The estimated maximum levels are generally found to be in good agreement with the actual levels. Again the maximum values based on $\langle|R_1|\rangle_{median}$ give slightly higher, more correct estimates than those based on $\langle|R_1|\rangle_{mean}$.

4. COUPLING LOSS FACTORS

The quantity $\langle|R_1|\rangle_{median}$ expresses the average ratio of reflected to incident wave amplitude for a system consisting of two finite beams. Thus, indirectly it represents the net transmitted power P_1 for $N \geqslant 1$. It takes into account the fact that the power transmitted to beam 2 is partly transmitted back to beam 1. Consequently, the average net reflection can be employed to calculate coupling loss factors for use in SEA models which are valid even at low modal overlap. This will be demonstrated in section 4.2.

However, before proceeding to this subject it seems relevant to consider briefly the general behaviour of $\langle|R_1|\rangle_{median}$ and draw a comparison with the traditional way of estimating the coupling loss factor. The traditional coupling loss factor is based on a travelling wave approach and in the derivation it is assumed that the aforementioned retransmission effect is negligible. This approximation is permissible only for a high modal overlap.

4.1. HIGH MODAL OVERLAP

The two previous sections have been concerned with determination of $\langle|R_1|\rangle$, the average value of $R_1 \exp(-\mathrm{j}k_1 2l_1)$, when the phase θ is unambiguous and ambiguous, respectively. For a system consisting of two finite beams a transition between these two cases will occur when damping in beam 2 is increased. The general behaviour of $\langle|R_1|\rangle_{median}$ and the standard deviation for a system consisting of two finite beams is shown in Figure 15 for different ratios of N.

In the first region up to a value of $k_2 l_2 \eta/4 = 0{\cdot}17$, cf. equation (9), the phase will be unambiguous and the losses will be moderate. In the range of $k_2 l_2 \eta/4$ from 0·17 to approximately 1·5 the phase will be ambiguous. Above the value of 1·5, beam 2 will be so heavily damped that the average net reflection will equal the reflection coefficient for the joint, i.e., $\langle|R_1|\rangle = r_{12}$.

The travelling wave estimate for the coupling loss factor η_{12} for a one-dimensional systems is given as [1]

$$\eta_{12} = (C_{g1}/2\omega l_1)\tau_{12}, \tag{18}$$

where C_{g1} is the group velocity of waves in beam 1.

It has been demonstrated in reference [16] that equation (17) gives a correct estimate of the coupling loss factor η_{12} when the modal overlap factor M is relatively high: that is, $M \geqslant 1$, where $M = \omega\eta n(\omega)$ and $n(\omega)$ is the modal density. This criterion can also be expressed as $k_2 l_2 \eta/4 \geqslant \pi/2$. From Figure 15 it is seen that this condition corresponds to the region where $\langle|R_1|\rangle = r_{12}$: that is, the case where beam 2 is so heavily damped that no power is reflected back to beam 1. This observation agrees with equation (18) which was derived under the assumption that no transmitted power will be reflected back to the first beam.

4.2. LOW MODAL OVERLAP

In the following, the coupling loss factor η_{12} which describes the power transmission from element 1 to element 2 will be determined for a system like that consisting of two coupled finite beams as depicted in Figure 1. It is assumed that the power P_1 is injected into beam 1 while the second beam receives only the power P_{12} through the coupling between the two beams. Hence, P_{12} is the net transmitted power from beam 1 to beam 2. It is assumed that the phase θ is unambiguous, which means that the condition in equation (9) is fulfilled. The modal density of the first beam n_1 is assumed to be higher than or equal to the modal density of the second beam n_2, and hence $N \geqslant 1$. The coupling loss factor

η_{21} corresponding to $N < 1$ can then be calculated from the coupling loss factor η_{12} by use of the reciprocity relation: that is,

$$\eta_{12} n_1 = \eta_{21} n_2. \tag{19}$$

Thus, it is furthermore assumed that the coupling power proportionality is exact; see reference [17].

It has been shown in reference [18] that for moderate damping the response of a one-dimensional wave guide is independent of whether the damping is distributed or concentrated at the ends. The implication is that $\langle |R_1| \rangle_{median}$ can also be expressed as what might be termed a net coupling loss factor α_{12} as opposed to η_{12} which is a gross coupling loss factor. The net coupling loss factor α_{12} is calculated so that the attenuation through one round trip corresponds to the attenuation expressed by $\langle |R_1| \rangle_{median}$ for a single incidence on the coupling. Thus, the net coupling loss factor α_{12} can be found as

$$\alpha_{12} = -2 \ln \{ \langle |R_1| \rangle_{median} \} / k_1 l_1. \tag{20}$$

The net power transmitted to the second beam P_{12} can be written in a form equivalent to the one used for the dissipated power: that is,

$$P_{12} = \omega \alpha_{12} E_1 \qquad \text{for} \qquad \alpha_{12} \ll 1, \tag{21}$$

where E_1 is the total energy of beam 1. In equation (21) it is obviously assumed that α_{12} is a small quantity.

The net transmitted power P_{12} can also be found from the fundamental SEA equation as

$$P_{12} = \eta_{12} \omega \{ E_1 - (n_1/n_2) E_2 \}, \tag{22}$$

where E_2 is the total energy of the second beam and ω is the angular frequency. Strictly, the energies appearing in equation (22) are the uncoupled total energies and not the total coupled energies as employed here. Such uncoupled total energies are calculated from the properties of the clamped uncoupled elements and the velocities and displacements related to the coupled system: that is, when both elements are coupled and in motion. The total coupled energies are the real energies that can be measured on the coupled system. Thus, it is inherently assumed that the difference beween the two is minor [19].

The total energy of the second beam E_2 is related to the power dissipated from the second beam $P_{2,diss}$ through the loss factor η_2 as

$$P_{2,diss} = \eta_2 \omega E_2. \tag{23}$$

As the power dissipated from the second element $P_{2,diss}$ must equal the net transmitted power P_{12}, the coupling loss factor η_{12} can be determined as

$$\eta_{12} = \frac{\alpha_{12}}{1 - n_1 \alpha_{12} / n_2 \eta_2} \qquad \text{for} \qquad 1 > \frac{n_1 \alpha_{12}}{n_2 \eta_2}. \tag{24}$$

The condition imposed on equation (24) is equivalent to specifying that there must be a difference in modal energies, that is, $E_1/n_1 > E_2/n_2$. This situation can arise here, because the energies employed are the coupled energies. Instead of substituting the values for $\langle |R_1| \rangle_{median}$ in equation (24) it is more practical to combine equation (14) and equation (20) to yield

$$\alpha_{12} = (D_N / 2N) \eta_2. \tag{25}$$

Finally, substituting equation (25) into equation (24) gives the coupling loss factor η_{12} as

$$\eta_{12} = D_N \eta_2 / N(2 - D_N) \qquad \text{for } 2 > D_N. \tag{26}$$

From this it is seen that the coupling loss factor η_{12} at low modal overlap depends on the loss factor of the second element η_2, the coupling between the two elements and their physical properties as expressed by the factors D_N and N.

4.2.2. *Numerical example*

Consider the system depicted in Figure 16. The system consists of five beams of different lengths with identical wave numbers k_n and loss factors η_n all coupled via simple supports. The first beam is driven in 10 independent positions by a harmonic point force causing an input power of P_1.

The exact mean square velocities (spatial average) $\bar{v}_n^2$ were calculated for each of the five beams by solving 30 equations with 30 unknowns. In order to ease the comparison with the estimated mean square velocities the resulting spectra were averaged in the frequency domain. The averaging was performed by sweeping the spectra with a Hanning window with a width equal to half the frequency span. For each frequency, the spectrum was multiplied by the Hanning window and an average of the product was calculated on an energy basis.

The coupling loss factors between each beam-pair were calculated as described above. Table 1 lists the ratios N, constants D_N for $\langle |R_1| \rangle_{median}$ (cf. equation (14)) and coupling loss factors η_{qp} and η_{pq}.

In order to eliminate any uncertainty with regard to whether differences could be caused by an incorrect estimate of Y_{avg} or the prediction method, the average mobility Y_{avg} was calculated from the exact solution by averaging the real part of the point mobility over 10 randomly chosen positions on the driven beam. This was done for both values of the loss factors. The resulting spectra of $\mathrm{Re}\{Y_{avg}\}$ were then averaged using a Hanning window as described above and the input power was calculated as $P_1 = 1/2\ \mathrm{Re}\{Y_{avg}\}|F_0|^2$.

Figures 17 and 18 shows a comparison between the exact and the approximate mean square velocities $\bar{v}_n^2$ for each of the five beams for two different values of the loss factor, $\eta_2 = 0{\cdot}001$ and $0{\cdot}01$. Generally, the agreement is fine as the deviation between the exact results and the SEA results are within ± 2 dB. The major differences are found for the fourth and fifth beam and these discrepancies might be due to some slight periodicity which causes some of the modes to huddle together. The increase of the spatially averaged velocity at the low frequency end is caused by the above described averaging process of the input mobility. Contrary to the real mobility the frequency averaged mobility does not go towards zero for the frequency going towards zero.

Table 2 shows a comparison between coupling loss factors for the above system at 5 kHz calculated using different methods. The first column shows the coupling loss factor calculated using the method described herein which depends on the loss factor of the receiving beam but not on frequency. The second column is based on the traditional expression, cf. equation (18), which depends on frequency but not on the losses. The third column is based on the expression given by equation (62) in reference [20] which is derived analytically from an approximate wave model. This expression depends both on frequency and losses in both transmitting and receiving beams. The traditional coupling loss factor, second column, is known to overestimate at low modal overlap.

5. CONCLUDING REMARKS

In this paper a method has been outlined for calculation of an improved coupling loss factor that is valid at low modal overlap. The method is based on numerical calculation of the average ratio of the reflected wave to the incident wave at the junction between two coupled beams. The average ratio is dependent on the properties of the coupling and the Helmholtz numbers of the two beams but it is independent of the exact boundary conditions of the two non-coupled ends. The calculation scheme is not restricted by the strength of the coupling. In the calculations it has been assumed that the influence of the losses only varies slowly with frequency so that the losses can be considered constant during a period. For the region with low modal overlap, this leads to an improved coupling loss factor that is found to depend on the losses of the receiving beam and to be independent of frequency. Improved coupling loss factors has been calculated and employed in a traditional SEA model to predict the mean square response at low modal overlap of coupled beam elements with good accuracy. For application to more general systems, it should be mentioned that the method can be extended to handle two-dimensional systems such as plate assemblies as it has been done in reference [21]. However, as the wave fields at low modal overlap for plates seldom are diffuse, good SEA predictions will probably require that this method is combined with information about the directivity of the wave fields [22].

ACKNOWLEDGMENTS

The author wishes to thank Dr M. Ohlrich for valuable discussions and support, and the Danish Technical Research Council for funding parts of this work.

REFERENCES

1. R. H. Lyon and R. D. DeJong 1995 *Theory and Application of Statistical Energy Analysis*. London: Butterworth-Heinemann; second edition.
2. E. J. Skudrzyk 1987 *Acustica* **3**, 123–147. Understanding the dynamic behaviour of complex vibrators.
3. S. H. Crandall and R. Lotz 1971 *Journal of the Acoustical Society of America* **49**, 352–356. On the coupling loss factor in statistical energy analysis.
4. H. G. Davies 1973 *Journal of the Acoustical Society of America* **51**, 393–401. Power flow between two coupled beams.
5. H. G. Davies and M. A. Wahab 1981 *Journal of Sound and Vibration* **77**, 311–321. Ensemble averages of power flow in randomly excited beams.
6. H. G. Davies and S. I. Khandoker 1982 *Journal of Sound and Vibration* **84**, 557–562. Random point excitation of coupled beams.
7. B. R. Mace 1992 *Journal of Sound and Vibration* **154**, 289–319. Power flow between two continuous one-dimensional systems: a wave solution.
8. B. R. Mace 1992 *Journal of Sound and Vibration* **154**, 321–341. The statistics of power flow between two continuous one-dimensional subsystems.
9. B. R. Mace 1992 *Journal of Sound and Vibration* **159**, 305–325. Power flow between two coupled beams.
10. S. Finnveden 1995 *Journal of Sound and Vibration* **187**, 495–529. Ensemble averaged vibration energy flows in a three-element structure.
11. C. T. Hugin 1997 *Journal of Sound and Vibration* **203**, 563–580. A physical description of the response of coupled beams.
12. R. S. Langley 1989 *Journal of Sound and Vibration* **135**, 499–508. A general derivation of the statistical energy analysis equations for coupled dynamic systems.
13. L. Cremer, M. Heckl and E. E. Ungar 1988 *Structure-Borne Sound*. Heidelberg: Springer Verlag; second edition.

14. B. R. MACE 1992 *Journal of Sound and Vibration* **155**, 375–381. Conservation of energy and some properties of reflection and transmission coefficients.
15. A. J. KEANE and C. S. MANOHAR 1993 *Journal of Sound and Vibration* **168**, 253–284. Energy flow variability in a pair of coupled stochastic rods.
16. F. J. FAHY and A. D. MOHAMMED 1992 *Journal of Sound and Vibration* **158**, 45–67. A study of uncertainty in applications of SEA to coupled beam and plate systems. Part I: computational experiments.
17. B. R. MACE 1994 *Journal of Sound and Vibration* **178**, 95–112. On the statistical energy analysis hypothesis of coupling power proportionality and some implications of its failure.
18. P. W. SMITH, JR. 1982 *Journal of the Acoustical Society of America* **72**, 472–475. Distinctions between boundary and distributed damping in a waveguide with a cutoff frequency.
19. F. J. FAHY 1975 *Revue d'Acoustique* **33**, 10–25. L'analyse statistique energétique: une revue critique.
20. B. R. MACE 1993 *Journal of Sound and Vibration* **166**, 429–461. The statistical energy analysis of two continuous one-dimensional subsystems.
21. C. T. HUGIN 1996 *Report no*. 67, *Department of Acoustic Technology*, *Technical University of Denmark*. Energy distribution of structure-borne sound in three-dimensional structures.
22. R. S. LANGLEY and A. N. BERCIN 1994 *Philosophical Transactions of the Royal Society* **A346**, 489–499. Wave intensity analysis of high frequency vibrations.